ELSEVIER

Journal of Neuroscience Methods 107 (2001) 63–70

JOURNAL OF NEUROSCIENCE METHODS

www.elsevier.com/locate/jneumeth

# Evaluation of a stereotactic frame for repositioning of the rat brain in serial positron emission tomography imaging studies

Daniel J. Rubins *[,1], A. Ken Meadors, Simon Yee, William P. Melega, Simon R. Cherry[1]

*Department of Molecular and Medical Pharmacology, UCLA School of Medicine, 1833 Leconte Ave, CHS 28-115, Los Angeles, CA, USA*

Received 21 December 2000; received in revised form 5 March 2001; accepted 5 March 2001

**Abstract**

For serial imaging studies of the rat brain with positron emission tomography (PET), reproducible positioning of the head can facilitate spatial alignment of images and quantitative analysis. To achieve this aim, we constructed a plastic head frame and tested the positioning reproducibility on a high-resolution small-animal PET scanner, microPET. Two sets of ear bars, with tapers of either 18° (sharp) or 45° (blunt), were evaluated for their relative precision in securing the animal to the frame. For sequential positioning of an animal, average distances from the mean position of 0.51 mm (SD 0.41 mm) and 0.91 mm (SD 0.48 mm) were measured with the sharp and blunt ear bars, respectively. These results show that a rat brain can be reproducibly positioned using the frame, with a variation of position less than the spatial resolution of modern animal PET scanners. Brain regions of interest defined on one scan and copied across subsequent scans of a frame-repositioned animal resulted in an average coefficient of variation of 5.4% (SD 2.7%) using the sharp ear bars and 6.8% (SD 2.5%) using the blunt ear bars. This methodology has the potential to improve quantitative assessment for serial PET studies. 

*Keywords:* In vivo imaging of small animals; Positron emission tomography; Image data analysis; Imaging instrumentation; Rat model of disease; Neuroimaging; Stereotactic head holder

## 1. Introduction

A major advantage of imaging brain neurochemistry using positron emission tomography (PET) is that longitudinal studies can be obtained in vivo for an individual subject. The recent development of dedicated small-animal PET scanners has made it possible to conduct these studies in rats (Unterwald et al., 1997; Brownell et al., 1998; Hirani et al., 2000; Kornblum et al., 2000). For example, with PET the same animal can be examined before and after an intervention, in a within subject study design. Quantification of these PET data is often expressed for a region of interest (ROI) that corresponds to a distinct structure of the brain (e.g. striatum, hippocampus). However, for multiple studies, the apparent size and position of a structure may vary, even for serial scans of the same animal, due to differences in radiotracer uptake, statistical noise, blood flow, or other effects that change the appearance of the image. Additionally, the drawing of consistent ROIs across studies may not be possible if the biological activity of the structure of interest has been altered by an intervention between scans. All of these factors can contribute to imprecise ROI definition, leading to inconsistent measurements.

One solution to this problem is to align PET images of the same animal spatially, such that one set of ROIs may be used for all image sets of that animal. Ideally, this could be achieved by placing the rat brain in precisely the same position within the scanner for each scan. Reproducible positioning would also facilitate placement of brain structures of interest consistently within the field of view of the PET scanner, thereby maximizing overlap between data sets and minimizing truncation. This is particularly relevant for rat brain imaging with animal PET scanners that have a limited axial field of view ($< 25$ mm).

* Corresponding author.

*E-mail address:* drubins@mednet.ucla.edu (D.J. Rubins).

[1] Affiliated with the Crump Institute for Molecular Imaging, Department of Molecular and Medical Pharmacology, UCLA School of Medicine, 1833 Leconte Ave., CHS 28–115, Los Angeles, CA, USA.

0165-0270/01/$ - see front matter 
PII: S0165-0270(01)00352-1

To address the issue of reproducible positioning, we constructed a stereotactic frame designed to position the brain of an anesthetized rat precisely. The frame also ensures that the rat brain does not move during a PET study. The accuracy of this frame was then evaluated in a high-resolution small-animal PET scanner. To benefit from the use of this frame for PET data analysis, the precision of rat brain placement within the scanner should be such that between-study position changes have a minimal effect on the measurement of the tracer concentration within ROIs used across the studies. The absolute placement precision that is required is defined by the spatial resolution of the scanner.

## 2. Materials and methods

### 2.1. Frame design

The design of the stereotactic frame (Fig. 1) was adapted from a similar frame, previously developed by Myers et al. (1996). It is similar to frames used for standard rat surgical stereotactic procedures, except that this frame was constructed with plastic on a Plexiglas platform to reduce the attenuation and scatter of photons during PET scans. The use of plastics also allows for frame compatibility with MRI scanners. The frame can be attached directly to the bed of the microPET scanner.

To describe the variability associated with reproducible positioning of the rat brain, three orthogonal directions must be defined to describe changes of position relative to the scanner. The direction along the axis of the scanner will be referred to as the axial direction. The other directions are in the transaxial plane, and will be referred to as the transaxial-horizontal $T_x$, and the transaxial-vertical $T_y$ directions.

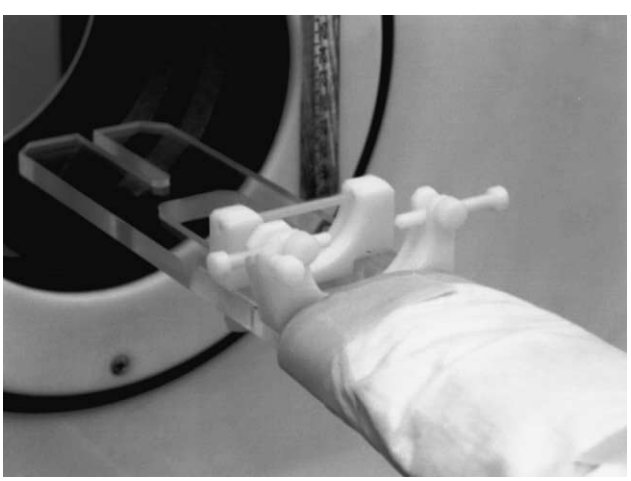

Fig. 1. The stereotactic frame attached to the microPET bed.

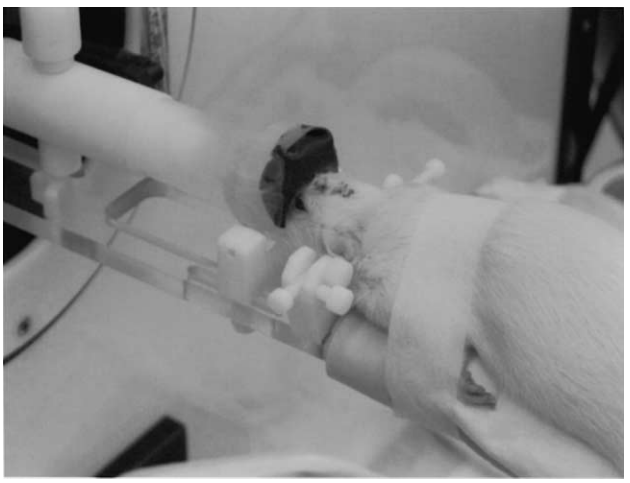

Fig. 2. Rats in the stereotactic frame are maintained on isofluorane for the duration of microPET studies.

For positioning of the rat in the frame, ear bars were inserted into the external auditory meatus of the animal to orient its interaural line. We evaluated two commonly used shapes of ear bars, one with a taper of 18° (sharp), and another with a taper of 45° (blunt). To facilitate reproducible positioning of the rat brain in the $T_x$ direction, one of the ear bars was constructed with three notches, restricting its placement to three discrete positions relative to the frame. A tooth bar for the upper incisors was fixed at 3.3 mm below the interaural line. For rats within the range of 250–350 g, this alignment of the animal head placed the brain in the orientation defined in the Paxinos–Watson atlas (Paxinos and Watson, 1986). The front end of the frame was designed to accommodate the use of gas anesthesia. The breathing apparatus from the gas anesthesia system can then be attached to the frame, and placed around the front of the rat head, while the mouth of the rat is around the tooth bar (Fig. 2).

### 2.2. microPET

The frame was tested in microPET, a dedicated small-animal PET scanner developed at UCLA (Cherry et al., 1997; Chatziioannou et al., 1999). The transaxial field of view of microPET is 112 mm, and the axial field of view is 18 mm. The microPET bed position is computer controlled in the axial direction. The scanner has a ring diameter of 172 mm. Using standard filtered back-projection (FBP) reconstruction, the resolution of the microPET scanner is 1.8 mm in all directions (Chatziioannou et al., 1999). An iterative 3D maximum a posteriori (MAP) reconstruction algorithm (Qi et al., 1998) was adapted for use with microPET, and resulted in improvements in resolution and noise characteristics of microPET images (Chatziioannou et al., 2000). microPET achieves volumetric spatial resolution of

1.5 mm in all directions with MAP reconstruction. Images of the rat brain acquired with this system allow the visualization of major structures (Fig. 3).

### 2.3. Frame evaluation experiments

To evaluate the accuracy of rat brain repositioning with the frame, a quantitative method is required to determine the position of the rat brain in the scanner. It was decided that the rat brain position could be measured by attaching point sources to the skull as fiducial markers, with the knowledge that the centroid of the image of a point source can be accurately located with an uncertainty much smaller than the spatial resolution of the scanner (Mintun et al., 1989). Accordingly, it was first necessary to determine the accuracy and reproducibility of measurements of the position of a point source obtained with microPET. For these preliminary studies, the location of a point source was measured in multiple trials without any movement between trials. Next, the point source was moved in increments as small as 0.1 mm to determine the sensitivity of the scanner to detect small position changes. Then, multiple trials consisting of removal and repositioning of the scanner bed within the scanner were obtained with a point source attached to the scanner bed. These studies allowed us to determine the sensitivity of the scanner to detect position changes, independent of the variance associated with the repositioning of the animal in the frame.

In the next set of studies, the location of fiducial markers that were attached to the skull of the living rat were measured in multiple trials, following the removal and repositioning of the rat within the scanner. Lastly, the reproducibility of rat brain positioning based on ROI consistency was evaluated at approximately 30 min following injection of $^{18}$F-2-fluoro-2-deoxyglucose (FDG). The distribution of FDG in the brain, after a suitable uptake period, reflects regional levels of glucose metabolism.

Animal care and procedures were in accordance with the 'Guide for Care and Use of Laboratory Animals' (National Institutes of Health publication 865-23, Bethesda, MD) and were approved by the UCLA Chancellor's Committee for Animal Research.

#### 2.3.1. Point source studies

To determine the precision of multiple measurements of the location of a point source of radioactivity, a point source (Ge-68, 0.3 MBq) with a diameter of 1 mm was placed in the microPET scanner. Twelve scans of 30 s duration were then acquired without any movement of the point source. Next, to determine if this method was sensitive to small changes in position, the point source was mounted on a translation stage within the microPET scanner, and stepped in distances of 0.1, 0.2, 0.3, 0.6, and 1.0 mm in the axial and $T_x$ direction. Six 30 s scans were acquired at each position. Following these experiments to confirm the accuracy and precision of the measurement of point source location, the reproducibility of positioning of the frame within the scanner was evaluated. This was measured by firmly mounting the point source on the frame, followed by the acquisition of 12 scans. After each scan, the bed was retracted from the scanner; the frame was physically detached and reattached to the scanner bed. Then the bed, by computer control, was moved back to the original bed position. The location of the point source within the scanner was determined for all experiments, using the methods described in Section 2.4.1.

#### 2.3.2. Fiducial marker study

For this study, Sprague–Dawley rats (250–350 g) were anesthetized with 100 mg/kg ketamine and 20 mg/kg xylazine. A midline incision between the bregma and interaural line was made on the scalp of each animal, and the surface tissue was retracted from the skull. Using a 1 mm diameter hand drill, indentations of approximately 0.5 mm were made into the bone surface of the cranium. Indentation positions were approximately 1.2 cm apart, with two positions directly located on the midline of the skull. The third position was made as far laterally as possible, forming a triangle with reference to each other. PVC tubes (Nalgene, Rochester, NY) with an inner diameter of 1 mm were affixed over each indentation with epoxy and all three tubes were permanently attached to the skull with dental acrylic.

On a subsequent day following attachment of the tubes (range 1–7 days), the rat was anesthetized as

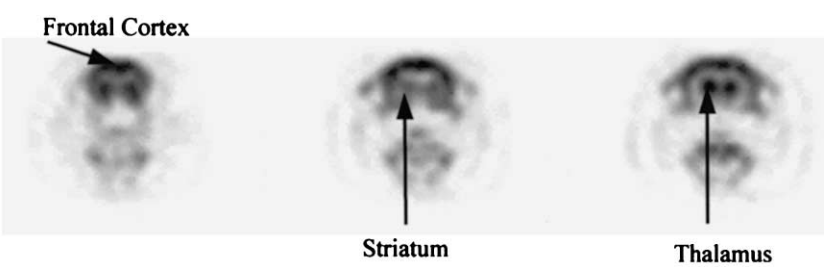


Fig. 3. FDG-PET images (summed activity between 45 and 85 min) representing glucose metabolism are presented for coronal planes of the rat brain showing frontal cortex, striatum, and thalamus.

described above. 1 μl of $^{18}F$ solution (1–3 MBq) was injected into the bottom of each PVC tube with a 10 μl Hamilton syringe. The rat was positioned in the frame by an investigator, and a preliminary scan was acquired to ensure that all three point sources of $^{18}F$ were within the scanner field of view. Following the scan, the frame was retracted from the scanner, and the rat was removed from the frame. The rat was then placed back in the frame by the same investigator, and the computer was used to place the bed in the same axial position. This procedure was repeated for the acquisition of a total of six scans. Five investigators who had prior experience placing rats in microPET with the stereotactic frame participated in this study. Each investigator performed this experiment with both types of ear bar. The location of each point source within the scanner was determined using the methods described in Section 2.4.2.

*2.3.3. FDG image study*

To measure the consistency of quantitative ROI measurements of an animal repositioned with the frame, a Sprague–Dawley rat was anesthetized as described above, and was injected via the tail vein, with FDG. After an uptake period of 30 min, the FDG distribution in the brain was assumed to be constant, as has been similarly shown with 2-[$^{14}C$]deoxyglucose (2-DG) (Mori et al., 1990). After the 30 min uptake period, four PET scans of 20 min duration were obtained. Between scans, the frame was retracted from the scanner, and the rat was removed from the frame, and repositioned for the next scan. This experiment was performed on two occasions, once with each set of ear bars. These images were evaluated using the methods described in Section 2.4.3.

*2.4. Image evaluation*

*2.4.1. Point source studies*

For evaluation of point source location, PET images were reconstructed with 3D filtered back-projection with cubic voxels of 0.29 $mm^3$. An analysis program was written in Interactive Data Language (Research Systems, Inc., Denver, CO, USA) to determine the centroid of the point source activity distribution, which was then used to define the location of the point source in the $T_x$, $T_y$, and axial directions. For the experiment where the point source was moved along a translation stage, the point source location measured by the analysis program was compared with that indicated by the translation stage. For the other two experiments, the mean location of the point source was determined. The average distance from the mean location was then calculated to indicate the magnitude of location changes for each experiment. These changes were characterized only in terms of the absolute 3D distance.

*2.4.2. Fiducial marker study*

The analysis program described in Section 2.4.1 was modified to determine the position of the three point sources in each PET image. As in Section 2.4.1, the distance of each point source from its mean location was determined. For each experiment, these values were averaged for all three point sources, to give an overall measure of the magnitude of the location changes of the rat brain. In addition, the overall average distance from the mean location was calculated across all experiments performed with each set of ear bars. As in Section 2.4.1, changes in location were characterized only in terms of absolute 3D distance. It was not determined if the position changes were due to rotation, translation, or a combination of the two.

*2.4.3. FDG image study*

These images were reconstructed using the MAP algorithm. To add and subtract the reconstructed FDG images for comparison, an intensity scaling factor was applied to the images based on the total number of detected events in each study. Pixel values are represented by arbitrary units. For each of the two experiments, the images were added, and all combinations of scans were subtracted. All addition and subtraction images were scaled identically, for both sets of studies, to allow for image comparisons between studies. In addition, regions of interest were drawn on the summed images, representing regions of the cortex and thalamus. These regions were copied onto each of the four scans, and the average pixel value within each region was determined. The coefficient of variance (COV) across scans was then calculated for each region.

## 3. Results

*3.1. Point source studies*

The average 3D distance from the mean measured location of a stationary point source that was imaged multiple times was 0.04 mm (SD 0.01 mm). The measured position changes primarily reflected the contribution of statistical fluctuations in the image data, and their effect on defining the position of the centroid of the point source. The results of stepping the point source through the scanner showed that changes in point source location as small as 0.1 mm are easily detected by this point source analysis method (Fig. 4a-b). The measured and true position values had a correlation coefficient of 1.00 in both the axial direction and the $T_x$ directions. The best fit slopes (ideal: 1.00) for the graphs were 1.04 (SD 0.03) for axial position changes and 0.98 (SD 0.01) for changes in the $T_x$ direction.

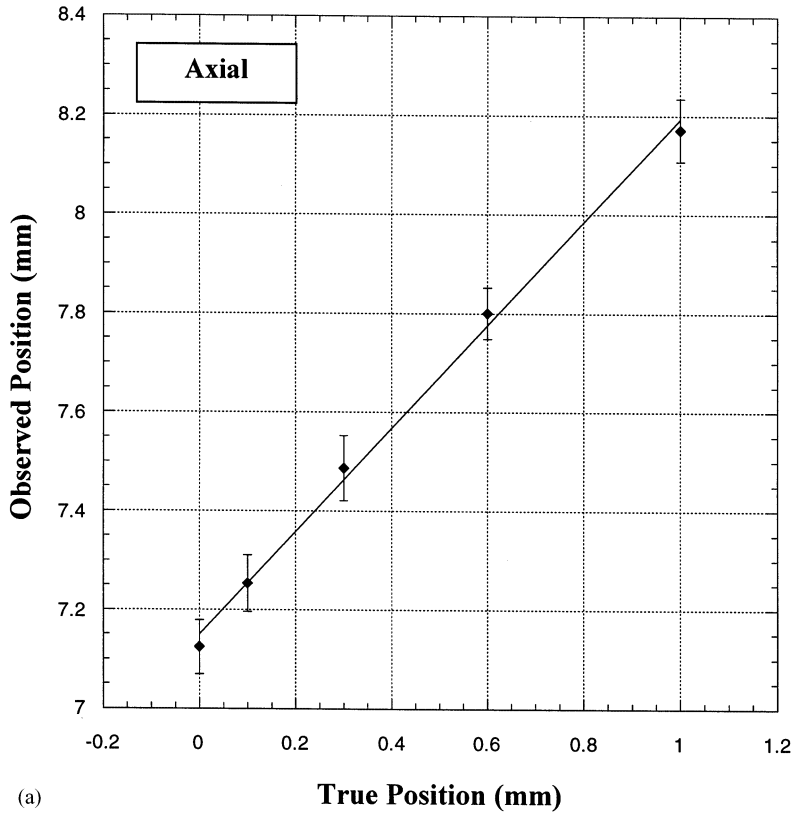


(a)

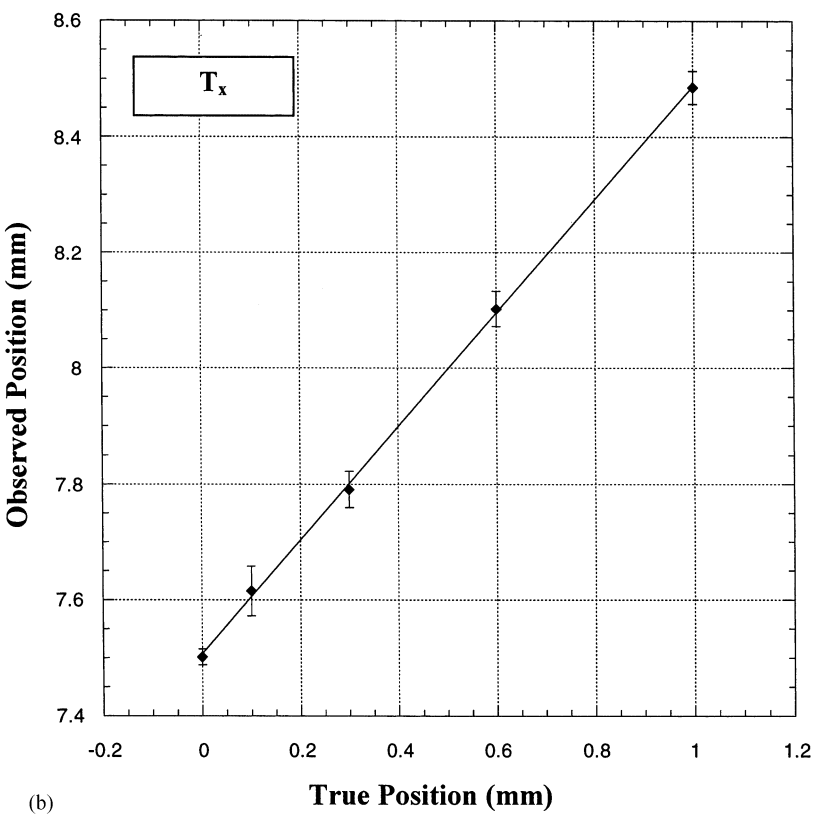


(b)

Fig. 4. The point source was stepped through the scanner in sub-millimeter increments in (a) the axial direction, and (b) the $T_x$ direction. The measured position of the point source is compared with the actual position of the point source for each step.

Table 1
The repositioning accuracy of the location of the rat brain is given for each investigator for blunt (45° taper) and sharp (18° taper) ear bars

| Investigator | Average distance from mean location (mm) |
|---|---|
| *Blunt (45° taper) ear bars* | |
| 1 | 1.15 (SD 0.68) |
| 2 | 1.04 (SD 0.26) |
| 3 | 0.87 (SD 0.48) |
| 4 | 0.99 (SD 0.39) |
| 5 | 0.49 (SD 0.18) |
| Overall | 0.91 (SD 0.48) |
| 95 % Confidence interval | [0.81, 1.01] |
| *Sharp (18° taper) ear bars* | |
| 1 | 0.69 (SD 0.22) |
| 2 | 0.28 (SD 0.12) |
| 3 | 0.27 (SD 0.10) |
| 4 | 0.86 (SD 0.71) |
| 5 | 0.44 (SD 0.09) |
| Overall | 0.51 (SD 0.41) |
| 95 % Confidence interval | [0.43, 0.60] |

The results of the frame-positioning experiment indicated that the average 3D distance from the mean measured location of the frame within the scanner was 0.16 mm (SD 0.16 mm). This distance is significantly smaller than the resolution of microPET ( $\sim$ 1.5 mm). The average distance from the mean location in the axial direction was only 0.04 mm (SD 0.03 mm), indicating that the computer-controlled bed positioning mechanism was not a major source of this variation.

### 3.2. Fiducial marker study

The results of the positioning experiment with the 45° (blunt) ear bars can be compared with those with the 18° (sharp) ear bars (Table 1). The average 3D distance from the mean measured location of the rat brain with the sharp ear bars was 0.51 mm (SD 0.41 mm), with a 95% confidence interval [0.43 mm, 0.63 mm]. The average with the blunt ear bars was 0.91 mm (SD 0.48 mm), with a 95% confidence interval [0.81 mm, 1.01 mm]. A two-tailed, paired $t$-test, based on the average distance from the mean location calculated for each investigator, confirmed that these differences between the two types of ear bar were statistically significant ($p < 0.05$).

### 3.3. FDG image study

The results of the FDG scans with blunt ear bars, the sum of these images, and all combinations of subtraction images are displayed in Fig. 5. The same information for the experiment performed with the sharp ear bars is displayed in Fig. 6. For each scan, the same coronal plane, near the center of the brain and the field of view, is displayed. In both cases, the major brain structures that appear in the individual scans are clearly visible in the summed image, indicating that position changes between scans were relatively small. In the subtracted images, visible brain structures indicate that a significant position change occurred between the scans. In both sets of experiments, scan 2 appears significantly displaced from its position in the other scans. ROIs that were copied across these sets of images had a COV of average pixel value of only 5.4% with the 18° ear bars, and 6.8% with the 45° ear bars. The results of individual structures are shown in Table 2.

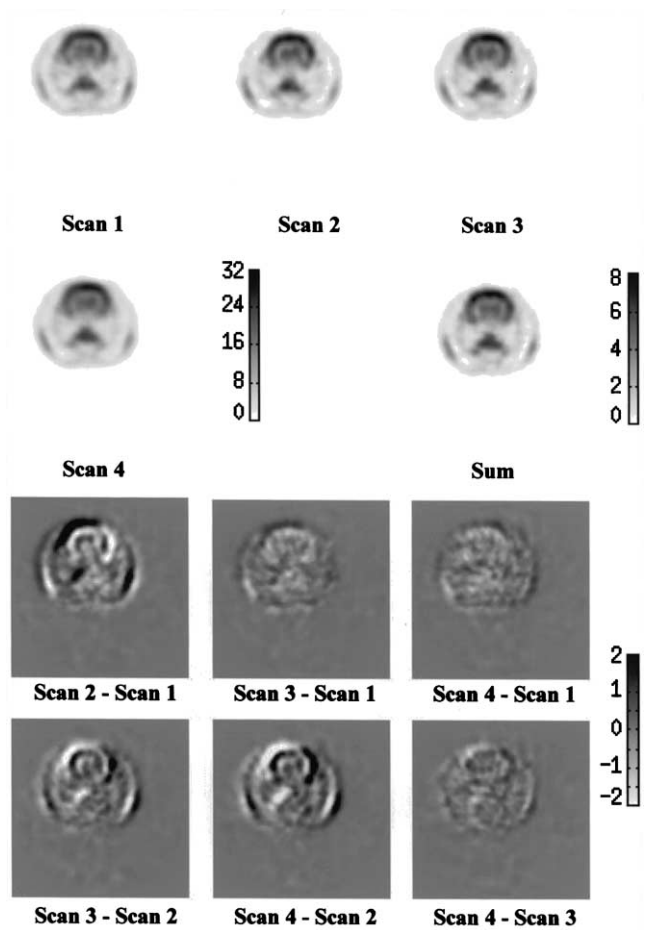


Fig. 5. A rat, injected with FDG (37 MBq, iv) was positioned within the scanner using the blunt (45° taper) ear bars, and scanned for 20 min. After removal of the animal from the stereotactic frame, it was repositioned in the same manner, and scanned for an additional 20 min. This procedure was repeated until four scans were obtained. One coronal slice is displayed from each of the four scans, along with the sum of all four scans, and all combinations of subtracted scans. Subtracted scans showing brain structures indicated that a significant position change occurred. In contrast, those with only a noise pattern, and no visible brain structures, indicate that good alignment was achieved. All pixel values are in normalized arbitrary units.

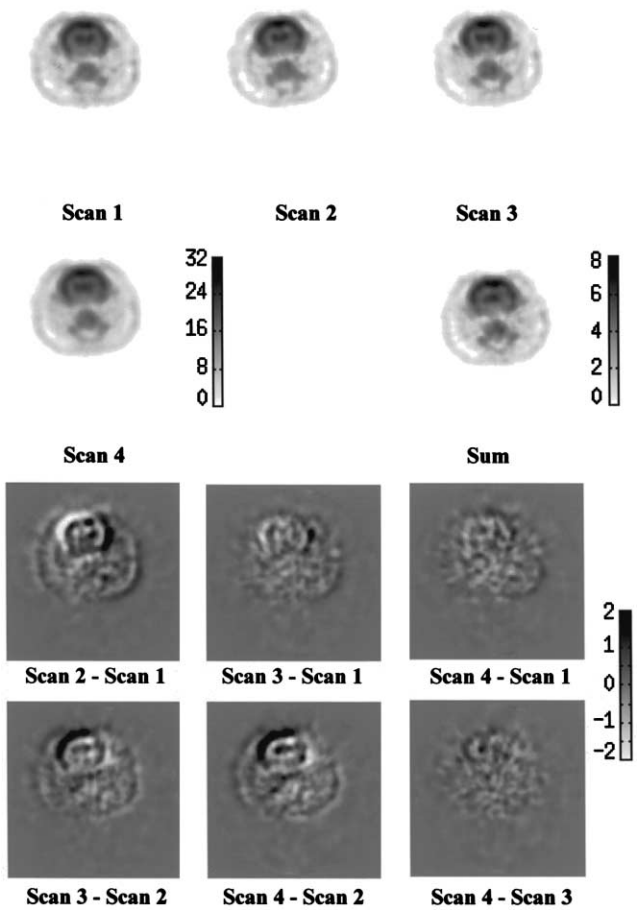


Fig. 6. Repositioning data for the sharp (18° taper) ear bars is displayed in the same format as Fig. 5.

## 4. Discussion

Many issues must be addressed in order to measure neurochemistry with quantitative accuracy using PET. A great deal of research is directed toward the development and validation of kinetic models for PET tracers, and toward obtaining accurate measures of radioactivity concentrations within the field of view of a PET scanner. Additionally, the accurate and reproducible definition of ROIs across studies is an important factor that can limit the accuracy of PET measurements. The stereotactic frame described in this report addresses this issue by facilitating the precise positioning of the rat brain within a PET scanner. This methodology allows for the same ROIs to be used across serial studies of an individual rat. In the future, it may be possible to use similar techniques for quantitative in vivo analysis of the mouse brain.

The results of the point source experiments confirmed that the location of a point source within microPET can be measured precisely, and that our method is sensitive to small changes in location. Further, the results show that the stereotactic frame can be positioned reproducibly within the scanner. The results of our evaluation of rat brain position demonstrate that better repositioning accuracy can be obtained by using the sharp ear bars rather than the blunt ear bars, and that the stereotactic frame can be used to accurately reposition the rat brain in microPET to sub-millimeter accuracy. Such a distance is within the practical spatial resolution of currently existing animal PET scanners (Lecomte et al., 1994; Bloomfield et al., 1995; Chatzioannou et al., 1999; Jeavons et al., 1999). However, it is unlikely that the reproducible positioning afforded by the stereotactic frame alone will be sufficient for studies using higher-resolution imaging techniques, such as MRI or X-ray computed tomography (CT). When greater repositioning accuracy is required than the frame can provide, image registration software can be used to align images (Woods et al., 1998). Nonetheless, the spatial alignment achieved with the use of the frame will likely contribute to the speed, accuracy, and robustness of subsequent image registration.

Table 2
For each set of FDG-PET scans, regions were drawn on a summed image and copied across the scans. The average pixel value within each region was calculated for each scan, and the coefficient of variance was determined

| Region | COV (SD/mean) (%) | |
|---|---|---|
| | 18° ear bars | 45° ear bars |
| Cortex | | |
| anterior | 5.3 | 7.5 |
| medial | 3.7 | 6.1 |
| posterior | 6.6 | 7.5 |
| Thalamus | | |
| anterior | 1.9 | 2.2 |
| right posterior | 5.0 | 7.6 |
| left posterior | 9.8 | 9.8 |
| Average | 5.4 | 6.8 |

## Acknowledgements

The authors wish to thank Linda Schultz and the staff of the animal PET and Biomedical Cyclotron for their assistance with these studies, Joe Gonzalez for assistance in frame development, A.J. Annala, Amy Moore, Keith Tatsukawa, and Dalia Araujo for their participation in positioning studies, Arion Chatziioannou and A.J. Annala for help with computer programming, Jim Sayre and Jim Mintz for assistance with statistical calculations, and Ralph Myers and Peter Bloomfield, MRC Cyclotron Unit, Hammersmith Hospital, for providing design drawings of their headholder. This work was supported, in part, by the United States Department of Energy contract DE-FC03-87-ER60615, and by a grant from the National Cancer Institute (RO1 CA69370).

## References


Bloomfield PM, Rajeswaran S, Spinks TJ, Hume SP, Myers R, Ashworth S, et al. The design and physical characteristics of a small animal positron emission tomograph. Phys Med Biol 1995;40:1105–26.

Brownell AL, Livni E, Galpern W, Isacson O. In vivo PET imaging in rat of dopamine terminals reveals functional neural transplants. Ann Neurol 1998;43:387–90.

Chatziioannou AF, Cherry SR, Shao Y, Silverman RW, Meadors K, Farquhar TH, et al. Performance evaluation of microPET: a high-resolution lutetium oxyorthosilicate PET scanner for animal imaging. J Nucl Med 1999;40:1164–75.

Chatziioannou A, Qi J, Moore A, Annala A, Nguyen K, Leahy R, et al. Comparison of 3-D maximum a posteriori and filtered backprojection algorithms for high-resolution animal imaging with microPET. IEEE Trans Med Imaging 2000;19:507–12.

Cherry SR, Shao Y, Silverman RW, Meadors K, Siegel S, Chatzioannou A, et al. MicroPET: a high resolution PET scanner for imaging small animals. IEEE Trans Nucl Sci 1997;44:1161–6.

Hirani E, Opacka-Juffry J, Gunn R, Khan I, Sharp T, Hume S. Pindolol occupancy of 5-HT(1A) receptors measured in vivo using small animal positron emission tomography with carbon-11 labeled WAY 100635. Synapse 2000;36:330–41.

Jeavons AP, Chandler RA, Dettmar CAR. A 3D HIDAC-PET camera with sub-millimetre resolution for imaging small animals. IEEE Trans Nucl Sci 1999;46:468–73.

Kornblum HI, Araujo DM, Annala AJ, Tatsukawa KJ, Phelps ME, Cherry SR. In vivo imaging of neuronal activation and plasticity in the rat brain by high resolution positron emission tomography (microPET). Nat Biotechnol 2000;18:655–60.

Lecomte R, Cadorette J, Richard P, Rodrigue S, Rouleau D. Design and engineering aspects of a high resolution positron tomograph for small animal imaging. IEEE Trans Nucl Sci 1994;41:1446–52.

Mintun MA, Fox PT, Raichle ME. A highly accurate method of localizing regions of neuronal activation in the human brain with positron emission tomography. J Cereb Blood Flow Metab 1989;9:96–103.

Mori K, Schmidt K, Jay T, Palombo E, Nelson T, Lucignani G, et al. Optimal duration of experimental period in measurement of local cerebral glucose utilization with the deoxyglucose method. J Neurochem 1990;54:307–19.

Myers R, Hume SP, Ashworth S, Lammertsma AA, Bloomfield PM, Rajeswaran S, Jones T. Quantification of dopamine receptors and transporter in rat striatum using a small animal PET scanner. In: Hume SP, Myers R, Cunningham V, Bailey D, Jones T, editors. Quantification of Brain Function Using PET. San Diego: Academic Press, 1996:12–5.

Paxinos G, Watson C. The rat brain in stereotaxic coordinates, second ed. Academic Press: Sydney, 1986.

Qi J, Leahy RM, Cherry SR, Chatziioannou A, Farquhar TH. High-resolution 3D Bayesian image reconstruction using the microPET small-animal scanner. Phys Med Biol 1998;43:1001–13.

Unterwald EM, Tsukada H, Kakiuchi T, Kosugi T, Nishiyama S, Kreek MJ. Use of positron emission tomography to measure the effects of nalmefene on D1 and D2 dopamine receptors in rat brain. Brain Res 1997;775:183–8.

Woods RP, Grafton ST, Holmes CJ, Cherry SR, Mazziotta JC. Automated image registration: I. General methods and intrasubject, intramodality validation. J Comput Assist Tomogr 1998;22:139–52.